Carcinogenesis vol.35 no.7 pp.1461–1468, 2014
doi:10.1093/carcin/bgu003
Advance Access publication January 7, 2014

Molecular basis of aflatoxin-induced mutagenesis—role of the aflatoxin B_1-formamidopyrimidine adduct

Ying-Chih Lin[1,2], Liang Li[3], Alena V.Makarova[4], Peter M.Burgers[4], Michael P.Stone[3] and R.Stephen Lloyd[1,5,*]

[1]Oregon Institute of Occupational Health Sciences and [2]Cancer Biology Program, Oregon Health & Science University, Portland, OR 97239, USA, [3]Department of Chemistry, Vanderbilt University, Nashville, TN 37235, USA, [4]Department of Biochemistry and Molecular Biophysics, Washington University School of Medicine, St. Louis, MO 63110, USA and [5]Department of Molecular and Medical Genetics, Oregon Health & Science University, Portland, OR 97239, USA

*To whom correspondence should be addressed. Tel: +503 494 9957; Fax: +503 494 6831;
Email: lloydst@ohsu.edu

Aflatoxin B_1 (AFB_1) is a known carcinogen associated with early-onset hepatocellular carcinoma (HCC) and is thought to contribute to over half a million new HCCs per year. Although some of the fundamental risk factors are established, the molecular basis of AFB_1-induced mutagenesis in primate cells has not been rigorously investigated. To gain insights into genome instability that is produced as a result of replicating DNAs containing AFB_1 adducts, site-specific mutagenesis assays were used to establish the mutagenic potential of the persistent ring-opened AFB_1 adduct, AFB_1-formamidopyrimidine (AFB_1-FAPY). This lesion was highly mutagenic, yielding replication error frequencies of 97%, with the predominant base substitution being a G to T transversion. This transversion is consistent with previous mutational data derived from aflatoxin-associated HCCs. *In vitro* translesion synthesis assays demonstrated that polymerase (pol) ζ was the most likely candidate polymerase that is responsible for the G to T mutations induced by this adduct.

Introduction

Chronic dietary exposure to aflatoxin B_1 (AFB_1), through the consumption of food products contaminated with the fungi *Aspergillus flavus* and/or *A. parasiticus*, is a significant risk factor for the development of early-onset hepatocellular carcinoma (HCC). HCC is the third leading cause of cancer death worldwide, with distinct geographical distributions, mainly in sub-Saharan Africa and Southeast Asia where concomitant risk factors frequently include both hepatitis B virus infection and AFB_1 exposure (1–3).

The biological basis of AFB_1-related HCC has been ascribed in part to the genotoxic and mutagenic effects of AFB_1. Upon metabolic activation by cytochrome P450 enzymes (4), AFB_1 is converted to the highly reactive intermediate AFB_1-8,9-epoxide (5), which can covalently bind to the N7 atom of deoxyguanosine in DNA to form the AFB_1-DNA adduct, 8,9-dihydro-8-(N7-guanyl)-9-hydroxyaflatoxin B_1 (AFB_1-N7-Gua) (6–9). In addition to spontaneous depurination, under slightly basic and physiological conditions, the AFB_1-N7-Gua adduct rearranges to the open-ringed AFB_1-formamidopyrimidine (AFB_1-FAPY) adduct. This lesion is the persistent AFB_1-DNA adduct in humans and animal models (10–13) (Figure 1A). Mutational analyses using several *in vitro* and *in vivo* model systems have revealed that the predominant mutations induced by AFB_1 exposure are G to T transversions (14–19). Further, in more than half of the HCC patient samples that were obtained from geographic locations with known high AFB_1 exposures, DNA sequence analyses revealed a G to T mutation at the third position of codon 249 in the *p53* tumor suppressor gene (20,21). Mutagenesis studies in SOS-induced *Escherichia coli*, which utilized site-specifically modified DNAs containing either the AFB_1-N7-Gua or AFB_1-FAPY adducts in a shuttle vector, demonstrated that both AFB_1-N7-Gua and AFB_1-FAPY adducts were promutagenic with mutation frequencies of 4 and 32%, respectively, and that both types of lesions caused predominantly G to T transversions (22,23). Based on its persistence in animal tissues, it is of particular interest to determine the mutagenic property of AFB_1-FAPY adducts in primate cells.

When mammalian cells replicate DNA that contains residual DNA damage induced both endogenously and exogenously, the majority of these adducts block high-fidelity replicative polymerases (i.e. pol δ and ε) and thus, cells utilize specialized DNA polymerases, known as translesion synthesis (TLS) polymerases to directly replicate past the damaged nucleotides. TLS polymerases not only possess flexible active sites to accommodate abnormal base alterations, but also lack

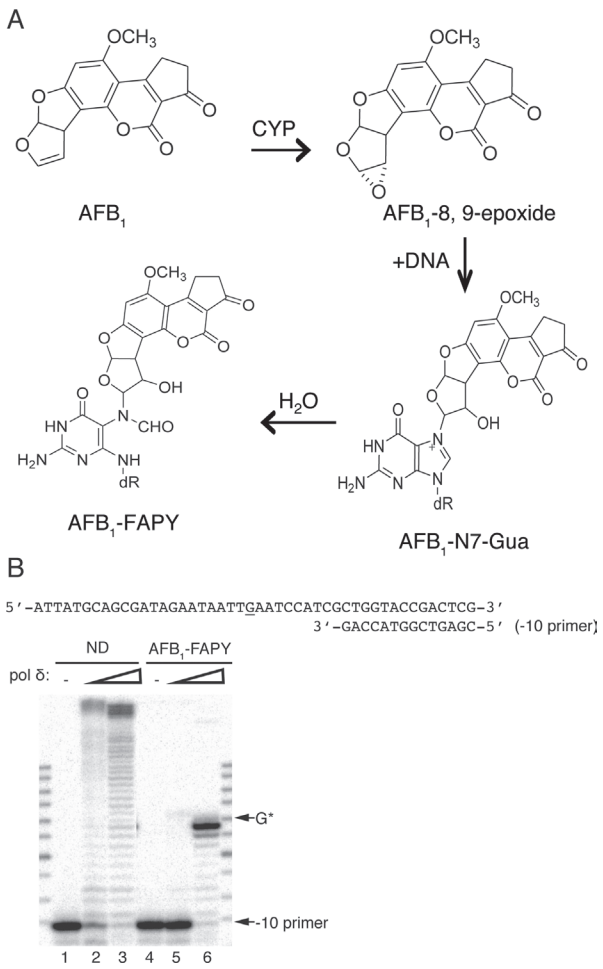

Fig. 1. (**A**) Formation of the AFB_1-DNA adducts. AFB_1 is metabolically activated to AFB_1-8,9-epoxide, which interacts with deoxyguanosine to form the cationic AFB_1-N7-Gua; further hydrolysis gives rise to AFB_1-FAPY. (**B**) Replication blockage of pol δ by AFB_1-FAPY. −10, oligodeoxynucleotide primers were annealed to ND or AFB_1-FAPY-containing DNA templates. Primer extensions were catalyzed by 1 nM (lane 2, 5) or 50 nM (lane 3, 6) pol δ in the presence of 100 μM dNTPs. G*, adducted site.

Abbreviations: AFB_1, aflatoxin B_1; AFB_1-N7-Gua, AFB_1-DNA adduct, 8,9-dihydro-8-(N7-guanyl)-9-hydroxyaflatoxin B_1; dA, deoxyadenosine; dG, deoxyguanosine; dNTP, deoxynucleoside triphosphate; FAPY, formamidopyrimidine; HCC, hepatocellular carcinoma; ND, non-damaged; ss, single-stranded; TLS, translesion synthesis.

proofreading exonuclease activities to remove potential misinsertions. As a result, the bypass of damaged nucleotides by TLS polymerases may lead to mutations. This process has been recognized to play a significant role in spontaneous and damage-induced point mutagenesis. The conservation of TLS polymerases across all three domains of life highlights their functional role in DNA damage tolerance and the maintenance of genome stability. Five eukaryotic TLS polymerases have been studied extensively, including pol ζ in the B family and members of the Y family: pol κ, η, ι and REV1 (24–28). Depending on the types of DNA damage, each polymerase may have distinct and/or similar bypass abilities. The insertion opposite a lesion and extension from the inserted nucleotide can be carried out by a single TLS polymerase alone, or through a concerted effort of different combinations of two TLS polymerases, followed by a reversion to normal replicative polymerase downstream of the damaged nucleotide (26,29,30). For example, pol η can bypass the ultraviolet-induced *cis-syn* T-T cyclobutane pyrimidine dimer accurately and efficiently (31,32), but in the absence of pol η, replication bypass of cyclobutane pyrimidine dimers has been suggested to be catalyzed by pol κ and/or ι in combination with pol ζ in an error-prone manner (33,34).

The molecular mechanism of AFB_1-induced mutagenesis has not been fully investigated. Banerjee *et al.* (35) reported that the archaea *Sulfolobus solfataricus* DNA polymerase IV (Dpo4), a homolog of human pol κ, can bypass AFB_1-FAPY in an error-prone manner *in vitro*. The goals of the current study were to investigate both the spectra and frequency of mutations generated following the replication of single-stranded (ss) DNAs containing a site-specific AFB_1-FAPY adduct in primate cells. By using a ss vector that prohibited any repair prior to TLS, it was possible to assess the replication fate of these adducts and infer the underlying mechanisms of replication bypass of AFB_1-FAPY adducts using *in vitro* replication assays.

Materials and methods

Materials

COS-7 cells were purchased from the American Type Culture Collection. The pMS2 shuttle vector was a generous gift from Dr Masaaki Moriya (State University of NY, Stony Brook, NY). Uracil DNA glycosylase, T4 DNA polymerase, T4 polynucleotide kinase, T4 DNA ligase and EcoRV were obtained from New England BioLabs. [γ-^{32}P]ATP was purchased from PerkinElmer Life Sciences. Bio-Spin columns were obtained from Bio-Rad. Amicon Ultra centrifugal filter devices were purchased from Millipore. Human pol κ, ι and yeast pol ζ were obtained from Enzymax, LLC. Human pol η catalytic cores were kindly provided by Dr Robert Eoff (University of Arkansas). Wild-type and the exonuclease-deficient form of *Saccharomyces cerevisiae* pol δ holoenzymes were purified as described previously (36). Dulbecco's modified Eagle's medium, Opti-MEM (reduced serum medium), L-glutamine, antibiotic–antimycotic, and Lipofectin reagent for tissue culture and *E. coli* Max Efficiency DH5α cells were purchased from Invitrogen. Phosphate-buffered saline and 100 mM deoxynucleoside triphosphates (dNTPs) were purchased from GE Healthcare Life Sciences. All other general reagents and chemicals were purchased from Fisher and Sigma–Aldrich.

Oligodeoxynucleotides

A 12mer oligodeoxynucleotide (5′-ATAATTXAATCC-3′) containing an AFB_1-FAPY adduct (Figure 1A) as designated by X was prepared as described previously. Non-damaged (ND) oligodeoxynucleotides (12 and 46mers) and primer DNAs were purchased from Integrated DNA Technologies.

Site-specific mutagenesis assay

Oligodeoxynucleotides (12mers) containing a site-specific AFB_1-FAPY or ND deoxyguanosine (dG) were inserted into ss pMS2 shuttle vector, as described previously (37–39). Briefly, a 44mer scaffold DNA was synthesized to be perfectly complementary to the linearized vector sequences following EcoRV cleavage of the spontaneously formed duplex hairpin, such that all positions of thymine were substituted with uracil nucleotides (5′-CUCGAGGGCCCCUGCAAGCGAU**GGAUUCAAUUAU**AUCGCU GGUACCGAGCUCGAAUUC-3′). The central 12 nucleotides (in bold) were complementary to the control and adducted DNAs to be inserted. The ss circular pMS2 DNA (15 pmol) was digested with EcoRV, followed by the addition of scaffold DNAs at equal molar concentrations to form the partially gapped duplex. The 12mer (15 pmol) was then annealed into the gapped duplex, and ligation was carried out at 12°C for >48 h. Scaffold and linear DNA fragments were eliminated by uracil DNA glycosylase and T4 DNA polymerase treatments in the absence of dNTPs.

Transfection of COS-7 cells, extraction of progeny DNA, *E. coli* transformation and differential hybridization analyses were carried out as described previously (38,39) with minor modifications. Following isolation of the replicated DNAs, progeny plasmids were used to transform *E. coli* DH5α according to the manufacturer's protocols (Invitrogen). Aliquots of bacterial cultures were grown in 96-well plates, lysed with 0.25 N NaOH and applied to a Hybond membrane using a vacuum manifold apparatus. The membranes were pH neutralized and washed, followed by the DNA being cross-linked to the membrane using a UV Stratalinker. To determine the mutation spectrum at the adducted site, differential hybridizations were conducted with a series of 5′-radiolabeled probes (5′-GATATAATTN AATCCATCGCTT-3′, where N refers to G, T, A or deletion) at 44°C overnight. A bridge oligodeoxynucleotide probe (5′-ATCCATCGCT TGCAGGGG-3′) was synthesized to be complementary to the sequence at the junction of the vector and insert and it was used to confirm the proper insertion of the control or adducted 12mers. The interpretation of the data from the differential DNA hybridization analyses were confirmed by direct DNA sequencing. DNAs that hybridized with the bridge probe, but not with any of the mutation or deletion probes, were further analyzed by DNA sequencing at the DNA Services Core at Oregon Health & Science University.

Construction of site-specifically modified linear templates for in vitro replication assays

Linear ss template DNAs (46mers) containing a site-specific AFB_1-FAPY were generated according to a previously reported procedure (38) with the following modifications. Briefly, the 12mer oligodeoxynucleotides (400 pmol) containing AFB_1-FAPY were centrally ligated between equal molar concentrations of a 16mer (5′-ATTATGCAGCGATAGA-3′) and an 18mer (5′-ATCGCTGGTACCGACTCG-3′) at the 5′ and 3′ end, respectively. These three DNAs were sequentially ordered by hybridization to a 42mer scaffold DNA (5′-AGTCGGTACCAGCGATGGATTCAATTATTCTATCGCTGCATA-3′). The 5′ end of an 18mer was ^{32}P labeled for purposes of purification of the full-length product. Reactions were performed using 800 units of the T4 DNA ligase at 20°C overnight. The ligated products were separated from all other reactant DNAs by electrophoretic separation through 10% acrylamide denaturing gels containing 8 M urea. DNAs that migrated at the correct size were cut from the gel and extracted using 0.5 M ammonium acetate/10 mM magnesium acetate buffer, desalted with water and concentrated by Amicon 3k centrifugal filter devices. The sequence of the ligation product 46mer was: 5′-ATTATGCAGCGATAGAATAATTGAATCCAT CGCTGGTACCGACTCG-3′, where the underlined G is AFB_1-FAPY.

In vitro *DNA replication assay*

Oligodeoxynucleotide primers were synthesized to be complementary to several positions within the 46mers such that the 3′ end of each primer was designed to hybridize 10 or 1 nucleotide upstream from the lesion site (−10 and −1 primers, respectively), immediately opposite the adduct (0 primer) or 2, 3 or 5 nucleotides downstream of the lesion site (+2, +3 or +5 primers, respectively). Three additional variations of the 0 primer were also synthesized to contain a mismatched nucleotide (A, T or G) at the 3′ end (0-A, 0-T, 0-G primers, respectively). The sequences of each of these primers appear as figure insets. The primers were ^{32}P labeled and annealed to the 46mer template at a 1:2 molar ratio in the presence of 40 mM NaCl, heated at 90°C for 2 min and cooled to room temperature. *In vitro* primer extension reactions were carried out using 5 nM primer–template complex in 25 mM Tris-HCl (pH 7.5), 8 mM $MgCl_2$, 10% glycerol, 100 μg/ml of bovine serum albumin and 5 mM dithiothreitol at 37°C for 30 min unless otherwise specified in the figure legends. Concentrations of dNTP(s) and polymerases are given in the figure legends. The reactions were terminated by the addition of an equal volume of a solution containing 95% (vol/vol) formamide, 20 mM ethylenediaminetetraacetic acid, 0.02% (wt/vol) xylene cyanol and 0.02% (wt/vol) bromophenol blue. Reaction products were resolved by electrophoresis through 15% acrylamide denaturing gels containing 8 M urea and visualized using a PhosphorImager screen.

Results

Mutagenic potential of AFB_1-FAPY adducts in primate cells

To evaluate the mutagenic potential of the AFB_1-FAPY adduct (Figure 1A) in primate cells, site-specific mutagenesis assays were carried out by transfecting a ss shuttle vector that had been engineered to contain a site-specific AFB_1-FAPY adduct or control ND dG, into African green monkey kidney COS-7 cells. Since the input DNA was

exclusively ss, DNA repair mechanisms were not operational until DNA replication bypass was complete. Following a 48 h incubation to allow replication of the shuttle vector, the resultant progeny plasmids were extracted and transformed into DH5α *E. coli* cells. Following selection for ampicillin resistance and growth of individual colonies, DNAs were extracted and analyzed for mutation spectra and frequencies by differential hybridization strategies. To assure that the control and adduct-containing 12mer DNAs had been correctly inserted into the shuttle vector, progeny plasmid DNAs were hybridized with an oligodeoxynucleotide bridge probe, spanning both the 12mer insert and the vector. Replicates of these DNAs were also hybridized with oligodeoxynucleotide probes that would only recognize the 12mer sequences surrounding the adducted site with perfect complementary. Thus, using stringent differential hybridization conditions, a mutagenic spectrum could be inferred. To confirm the accuracy of the differential hybridization results, representative colonies were picked for DNA sequencing to verify the correct identification of the mutation by each sequence-specific probe. All plasmid DNAs that hybridized only with the bridge probe, indicating the presence of the adducted oligodeoxynucleotide insert, but not with any sequence-specific mutation probes, were subjected to DNA sequencing to determine the sequence of the progeny DNA.

Analyses of these data revealed that the mutation frequency was exceptionally high, in which 97% of the translesion bypass events for the AFB_1-FAPY adduct led to a mutagenic outcome (Table I). No mutations were detected with the control ND sequence (Table I). The mutation spectrum included single base substitutions and deletions. The predominant mutations that were introduced as a result of replicating past the AFB_1-FAPY adducts were G to T transversions, accounting for 86% of all mutations scored, followed by a much lower frequency of G to A transitions (~10%), even less frequent G to C transversions and deletions that accounted for <3% of the total events observed. Overall, these data demonstrate that replication of DNAs containing an AFB_1-FAPY adduct in primate cells was highly mutagenic. The predominant G to T transversion strongly agrees with previously reported mutational analyses of HCC patient samples from regions known for high aflatoxin exposure (20,21).

AFB_1-FAPY blocks replicative pol δ

Since the mutagenesis data described above demonstrated that DNA polymerases in COS-7 cells could bypass the AFB_1-FAPY adduct, an investigation was initiated to identify which of the replicative or TLS DNA polymerases could be responsible for the cell-based mutagenesis. Although these are very large lesions that would be anticipated to block replicative DNA polymerases, yeast replicative DNA polymerase δ was analyzed for its capacity to catalyze replication past the biologically stable AFB_1-FAPY adduct. *In vitro* replication assays were designed to measure bypass under running (−10 primer) start conditions (Figure 1B). Although pol δ efficiently extended the −10 primer on the ND template to full-length products, the presence of the AFB_1-FAPY adduct blocked extension of the primer at one and two nucleotides prior to the lesion, even at the highest concentration of pol δ tested (Figure 1B, compare lanes 3 and 6). Additionally, these data suggest that the efficiency of loading pol δ, even on the −10 primer may be impeded due to the presence of the adduct, since overall primer utilization was significantly decreased (Figure 1B, compare lanes 2 and 5). Furthermore, there was no detectable full-length bypass product of AFB_1-FAPY. These results demonstrated that AFB_1-FAPY represents a strong replication block to pol δ.

Standing start single and combined dNTP reactions were also performed using a −1 primer. However, the exonucleolytic activity of pol δ dominated all polymerization reactions, with no nucleotide incorporation detected (Supplementary Figure 1A and B, available at *Carcinogenesis* Online). In addition, when an exonuclease-deficient form of pol δ (pol δ-Exo) was used, it poorly inserted all four dNTPs opposite the lesion and could extend from a mispaired A opposite AFB_1-FAPY-dG (note the band at +2 site in lane 2, Supplementary Figure 1C, available at *Carcinogenesis* Online). Comparative analyses of differences in nucleotide incorporation between pol δ and pol δ-Exo revealed that the proofreading function of the exonuclease prevented miscoding and synthesis past AFB_1-FAPY by pol δ.

Pol ζ-mediated replication bypass of AFB_1-FAPY leads to G to T mutation

Since pol δ (and by inference other replicative polymerases) could not bypass this lesion, investigations were designed to test the ability of DNA pol ζ to replicate past the AFB_1-FAPY adducts *in vitro*. As shown in Figure 2A, pol ζ preferentially inserted an A opposite the lesion, as evidenced by the extension product at the +2 site. This insertion of three nucleotides most likely represented an incorporation of deoxyadenosine (dA) opposite the adduct, followed by an additional synthesis of two nucleotides downstream (Figure 2A, lane 8). Furthermore, a full-length bypass product was observed when all dNTPs were added, demonstrating that AFB_1-FAPY can be bypassed by pol ζ (Figure 2A, lane 12). Analyses of single-nucleotide incorporation reactions with the ND template showed that as expected, pol ζ preferentially inserted a correct C, whereas A, G or T could also be utilized, albeit less efficiently (Figure 2A, lanes 2–5).

Next, the hypothesis that pol ζ could preferentially extend beyond a misincorporated A opposite the AFB_1-FAPY lesion was tested (Figure 2B). Extension reactions were conducted using primers with different 3′ end opposite the adducted nucleotide. Pol ζ preferentially extended the mispaired A primer when annealed to the damaged template (Figure 2B, lane 13). Using higher concentrations of pol ζ, it was possible to detect extension products off of all mispairs, but not from the non-mutagenic deoxycytidine (data not shown). Under conditions using the ND template, all primers were efficiently extended (Figure 2B, lanes 5–8).

Thus, our results constitute the first biochemical evidence that pol ζ can catalyze replication bypass of AFB_1-FAPY adducts by preferentially misincorporating dA opposite the lesion and extending beyond the misinsertion. These data suggest that pol ζ could be the major DNA polymerase responsible for the predominant G to T mutation induced by AFB_1-FAPY *in vivo* (Table I).

Replication bypass of AFB_1-FAPY by human pol κ, η and ι

To test whether members of the Y family TLS polymerases (pols κ, η and ι) could also contribute to the observed mutagenesis (Table I), the ability of these polymerases to catalyze replication bypass of the AFB_1-FAPY adduct was examined. Although primer extensions were readily detected on a ND template for all polymerases (Figure 3 and Supplementary Figure 2A–C, available at *Carcinogenesis* Online), when either human pol κ (Figure 3A) or η (Supplementary Figure 2A, available at *Carcinogenesis* Online) encountered the AFB_1-FAPY adduct, replication was stalled following insertion opposite the lesion. Additionally, pol κ-catalyzed replication showed major pause sites one and two nucleotides prior to the lesion (Figure 3A, lanes 5–6), whereas pol η also paused one nucleotide before and after the lesion

Table I. Mutation spectrum generated from replication bypass of AFB_1-FAPY adducts in COS-7 cells

DNA modification	Colonies scored	Mutated	Single base substitutions			Deletions	Other position substitution	Frequency of mutation (%)
			G to T	G to A	G to C			
ND	189	0	0	0	0	0	0	0
AFB_1-FAPY	203	197	170 (86.3%)	16 (8.1%)	5 (2.5%)	5 (2.5%)	1 (0.5%)	97

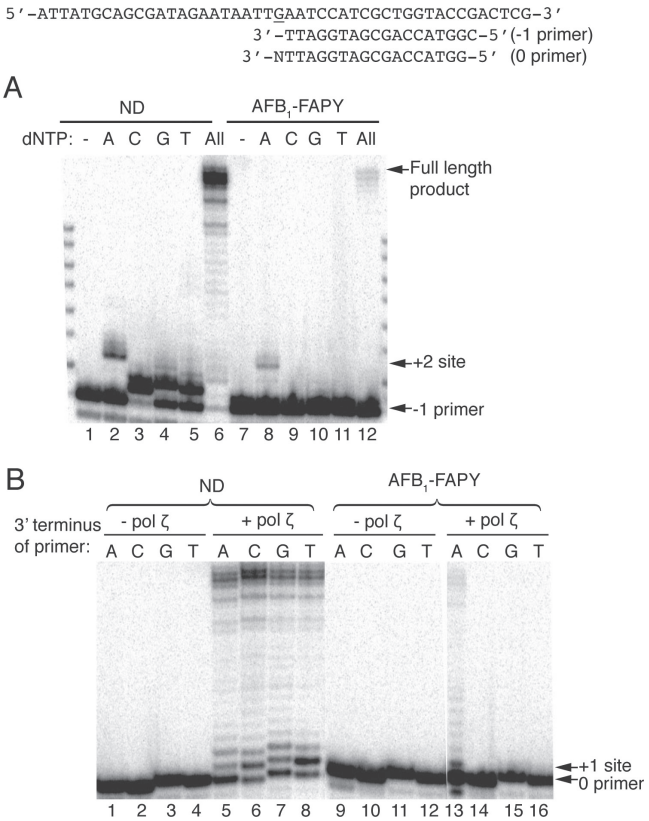

Fig. 2. Replication bypass of AFB_1-FAPY by yeast pol ζ. The −1 or 0 oligodeoxynucleotide primers with different 3′ end (where N represents either A, C, G or T) were annealed with ND or AFB_1-FAPY-adducted DNA templates. (**A**) Single-nucleotide incorporations and primer extension reactions were catalyzed by 5 nM (ND) or 50 nM (AFB_1-FAPY) pol ζ in the presence of 100 μM individual or all dNTPs. (**B**) Oligodeoxynucleotide primer extensions from the matched C or mismatched A, G and T 3′ terminus opposite ND or AFB_1-FAPY were catalyzed by 10 nM pol ζ in the presence of 100 μM dNTPs.

(Supplementary Figure 2A, available at *Carcinogenesis* Online, lanes 5–6). Similar to data shown for pol δ, both pol κ and η exhibited reduced loading and primer utilization on the adducted templates. Analyses of single-nucleotide incorporation reactions revealed that both pol κ and η could incorporate all dNTPs opposite AFB_1-FAPY, albeit inefficiently (Figure 3B, lanes 8–12 and Supplementary Figure 2B, available at *Carcinogenesis* Online, lanes 8–12, respectively). Further extensions beyond the lesion to +2 and/or +3 sites were observed when either deoxyadenosine triphosphate alone or all dNTPs were present in the reaction, with both pol κ and η, generating minute amounts of full-length bypass products when all four dNTPs were included in the reaction. Pol κ appeared to incorporate all four dNTPs with equal efficiency, whereas pol η preferentially incorporated purines over pyrimidines. Since these data do not match the observed mutagenic spectra, we consider that pol ζ is the most likely candidate for catalyzing the cellular bypass reaction.

To further examine the possible mechanism by which pol κ and η might contribute to G to T mutagenesis, primer extensions were carried out using four 0 primers, that contained a matched or mismatched nucleotide at the 3′ end opposite the lesion. It was hypothesized that preferential primer extension would occur from the mispaired A, thus accounting for the mutagenic outcome. Pol κ extended mismatched A primers that had been annealed to the damaged template somewhat more efficiently than the corresponding mismatched G or T primers, whereas the correct C primer was not extended (Figure 3C). As anticipated, correctly matched C primers that had been annealed to the ND template were efficiently utilized. In contrast, pol η more efficiently extended matched C primers than corresponding mismatched A, G or T primers when annealed to either ND or damaged templates (Supplementary Figure 2C, available at *Carcinogenesis* Online). To further rule out a significant role for pol η in the bypass of this adduct, pol η-deficient COS-7 cells were generated by short hairpin RNA against *Pol η* and were used in the mutagenesis assay as described above [in collaboration with I.G.Minko (OHSU), R.W.Sobol (University of Pittsburgh) and T.G.Wood (University of Texas Medical Branch), unpublished]. No changes were detected in the AFB_1-FAPY mutation frequency or spectrum in pol η-depleted COS-7 cells compared with wild-type cells (data not shown). Collectively, these data suggest that human pol κ and η may only exert a limited role in cellular replication bypass of AFB_1-FAPY through either error-prone or error-free reactions.

Additionally, it was observed that human pol ι could not incorporate any nucleotides opposite AFB_1-FAPY, although it could extend matched C primers annealed to AFB_1-FAPY more efficiently than the corresponding mismatched A primers *in vitro* (data not shown). Taken together, these results suggest that polymerases κ, η and ι are unlikely to be the primary contributors (but may serve as backup TLS polymerases) for processing AFB_1-FAPY adducts *in vivo*.

Resumption of efficient replication by pol δ

To test how far beyond the lesion site normal replication can resume, primer extension reactions were carried out with pol δ using ND or AFB_1-FAPY-modified templates annealed to +2, +3 and +5 primers, containing either matched C or mismatched A opposite the lesion, mimicking the accurate and mutagenic bypass observed *in vivo* (Figure 4). When the correct C was positioned opposite control dG or an AFB_1-FAPY adduct, pol δ efficiently extended all primers (Figure 4A, lanes 4–9). However, for the lesion containing templates, there was a small percentage of the primer resected primarily back to the +1 site. Furthermore, the extension efficiencies increased as the number of correct base pairs beyond the lesion increased. All primers with the ND template were completely utilized.

In contrast to the data with the correct C opposite the lesion, when a mispaired A was positioned opposite the adduct for the +2 or +3 primer, the exonuclease activity digested back to the −1 position (Figure 4B, lanes 7–8). Appreciable amounts of full-length products were only obtained with the mispaired +5 primer (Figure 4B, lane 9). Even under these conditions, some +5 primers were resected to the −1 site. In contrast, mismatched primers that were hybridized to the ND template were fully extended (Figure 4B, lanes 4–6). Collectively, these data revealed that for pol δ, the balance between polymerization and exonucleolytic resection was affected by the location of the mispair in the duplex primer template. Thus, the balance between the exonuclease and polymerase activities shifted toward extension when the mismatch was located deeper in the duplex. These data suggest that the TLS polymerase(s) need to continue several nucleotides beyond the lesion to preserve the mutagenic bypass before switching to a replicative polymerase.

Discussion

Aflatoxin-associated HCCs represent an enormous global health crisis, with a significant percentage of the estimated 550 000–600 000 new cases of HCC per year attributed to aflatoxin exposure alone (40). However, insights into the molecular mechanisms driving this mutagenesis as an early event of hepatocellular carcinogenesis have not been elucidated in either non-human primate or human cells. In the current study, we addressed the following issues: (i) the mutagenicity of AFB_1-FAPY in primate cells using a site-specifically modified ss vector and (ii) the mechanism of replication bypass of AFB_1-FAPY adducts using *in vitro* replication assays catalyzed by eukaryotic replicative and TLS DNA polymerases δ, ζ, κ, η and ι.

The utility of pMS2 ss shuttle vector containing site-specific DNA adduct, combined with differential hybridization analysis, in mutagenesis studies of various carcinogens has been demonstrated

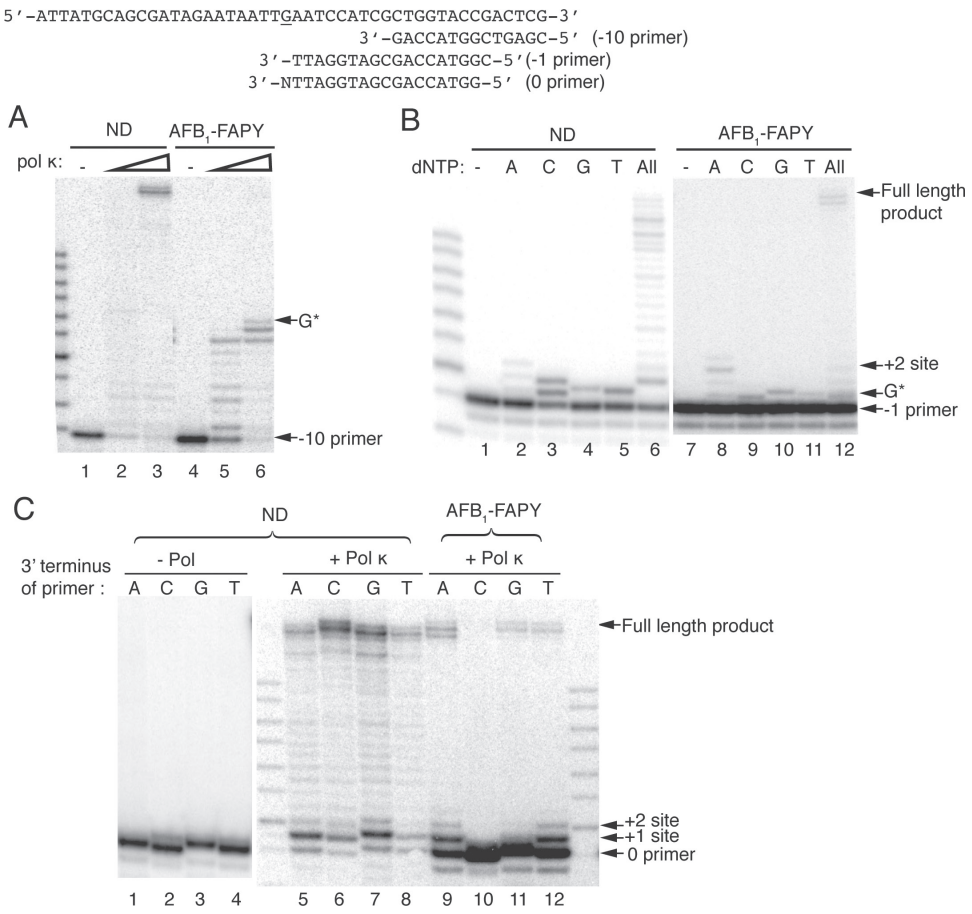

Fig. 3. Replication bypass of AFB_1-FAPY by human pol κ. Oligodeoxynucleotide primers (−10, −1 or 0) with different 3′ termini (designated as N, which represents either A, C, G or T) were annealed to ND or AFB_1-FAPY-containing DNA templates. (**A**) Primer extension reactions were catalyzed by increasing concentrations of pol κ (2 or 10 nM) in the presence of 100 μM dNTPs. (**B**) Single-nucleotide incorporation and primer extension reactions were conducted by 2 nM (ND) or 10 nM (AFB_1-FAPY) pol κ in the presence of 20 μM (ND) or 100 μM (AFB_1-FAPY) combined or individual dNTPs. (**C**) Primer extensions from the matched C or mismatched A, G, and T 3′ terminus opposite AFB_1-FAPY or ND were catalyzed by 10 or 0.5 nM pol κ in the presence of 20 μM dNTPs. G*, indicates the position of the adducted site.

by others and our laboratory (37–39,41,42). This approach allows straightforward detection of mutation spectrum and frequency opposite the lesion within a designated region of the vector, but without biased selection and interference from DNA adduct formation and DNA repair processes.

The results of our mutagenesis assays in primate cells were in good agreement with previous prokaryotic-based studies (23), indicating that AFB_1-FAPY is a biologically relevant mutagenic DNA adduct, predominantly giving rise to G to T transversions (Table I). These data also correlate well with previous observations of G to T transversions dominating the mutagenic spectrum of human AFB_1-associated HCC samples and in experimental model systems treated with AFB_1 (14,15,17,18,20,21,43). Taken together, these data suggest a causative role of AFB_1-FAPY in the initiation of liver cancer through mutagenesis. More strikingly, the mutagenicity of AFB_1-FAPY lesions in primate cells appeared to be much higher (97%, Table I) than that previously observed in *E. coli* cells (32%) (23). These data indicate that primate cells, and by way of extension to human cells, are more susceptible to the mutagenic effect of AFB_1 than *E. coli*, thus emphasizing the carcinogenic potency of AFB_1 in animals and humans.

A limitation of the present study was that only one DNA sequence context was examined. The immediate 5′ sequence context of the lesion was 5′ TT**G** in which the G in bold was the site of the adduct. In this specific sequence, there could be two competing hypotheses for the molecular mechanisms underlying the high frequency G to T transversions. The first is a simple misinsertion of dA opposite the adduct and subsequent extension from that mispair, followed by correct base pairing of the following two nucleotides, both dAs. This reaction could conceivably occur as a continuous processive reaction, or as a series of associative/dissociative polymerization steps in which the incorporation of nucleotides would be distributive. Alternatively, these data could also be anticipated if there was a transient DNA polymerase slippage mechanism in which the adducted nucleotide was expelled from the active site and the incorporation of dA would be opposite the 5′ unadducted deoxythymidine, followed by a slippage/realignment of the newly synthesized dA opposite the AFB_1-FAPY adduct. This would then be followed by normal base-pairing synthesis of the downstream sequences. This model could also possibly account for the G to T transversions. Of these two competing models, we favor the former for the following reasons. First, to the best of our knowledge, mutation hotspots have not been reported at G:C pairs that are adjacent to a run of consecutive deoxythymidines. Instead, AFB_1-induced G to T mutation sites frequently arise at the third base of codon 249 (AGG in human) of the *p53* tumor suppressor gene and the first or middle base of codon 12 (GGC in human or GGA in trout) of the *ras* oncogene (15,17,44). In addition, Besaratinia *et al.* (45) found that about half of the mutation sites of the predominant G to T transversions in the *cII* transgene in AFB_1-exposed Big Blue MEF cells occurred within CpG sequence contexts. Similarly, this sequence specificity was observed at nucleotide positions 101, 108, 115, 140, 208 and 320 as G to T mutation hotspots in the *gpt* gene in AFB_1-treated mouse liver (43). Therefore, it seems more likely that the G to T transversions detected in the current sequence context are caused by the combination of a misincorporated dA opposite the AFB_1-FAPY

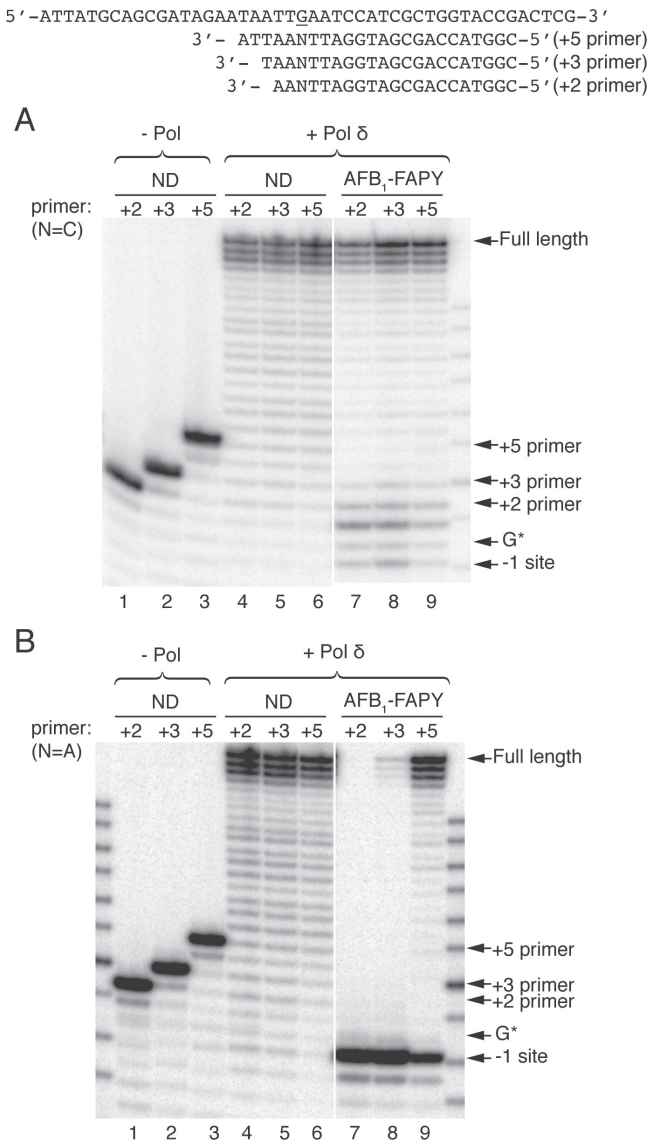

Fig. 4. Resumption of replication by pol δ downstream of AFB_1-FAPY. +2, +3 or +5 oligodeoxynucleotide primers with either matched C or mismatched A opposite the lesion or control site were annealed to ND or AFB_1-FAPY-containing DNA templates. (**A** and **B**) Primer extensions were catalyzed on matched and mismatched primers, respectively. All reactions were catalyzed by 50 nM pol δ in the presence of 100 μM dNTPs. G*, adducted site.

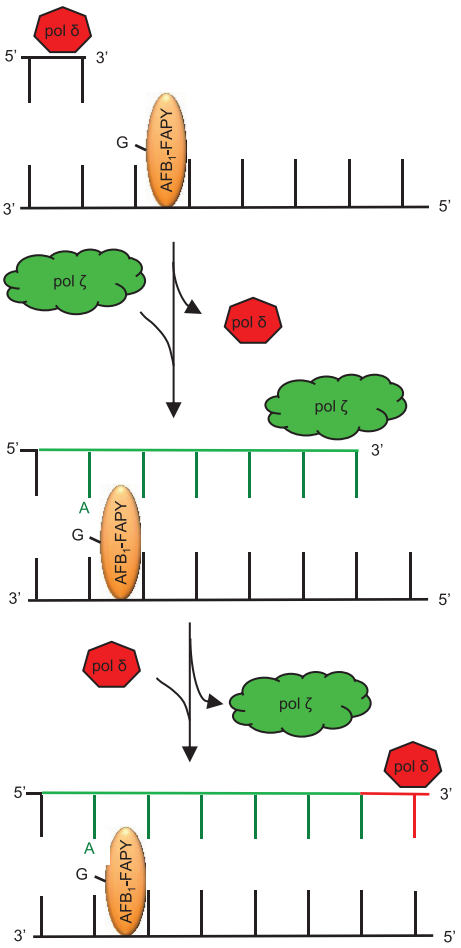

Fig. 5. Proposed model of TLS past AFB_1-FAPY. The mutagenic bypass of AFB_1-FAPY by pol ζ. The current model suggests that pol δ can synthesize up to one nucleotide prior to the lesion, followed by a polymerase switch to pol ζ. Pol ζ is proposed to preferentially insert an A opposite the lesion and extend synthesis several nucleotides downstream from the inserted A (indicated by dark green lines). This would be followed by a second polymerase switch to pol δ that catalyzes resumption of normal DNA replication.

lesion and extension from the misinsertion by DNA polymerase(s) as discussed below.

Systematic biochemical studies suggest a model of TLS across AFB_1-FAPY adducts (Figure 5). Upon encountering an AFB_1-FAPY adduct during replication, synthesis by the replicative polymerases (here represented by pol δ) are hypothesized to be blocked, resulting in a switch to pol ζ to insert an A opposite and extend beyond the lesion. This model predicts that, following synthesis of a short stretch of DNA, normal replicative polymerases could resume replication to preserve the mispair. A subsequent round of DNA replication would be required to make permanent the G to T mutation that occurred in our system with 97% probability. Although pol κ exhibited marginal preference for extending the mismatched A primer terminus, which could potentially contribute to G to T mutations, experimental proof of a combined two polymerase bypass mechanism using pol ζ and κ was not evident (data not shown). These data are also in accordance with the observation that pol ζ was involved in AFB_1-induced mutagenesis when human cytochrome P450 1A2 enzyme was expressed in yeast cells to metabolically activate AFB_1 (46).

As an overall trend, the DNA polymerases tested in the present study appeared to bypass AFB_1-FAPY adducts *in vitro* with minimal efficiency. Although REV1 and proliferating cell nuclear antigen have been shown to interact with these replicative and TLS polymerases to enhance their ability in processing certain DNA lesions (25), our results demonstrated the intrinsic actions of these DNA polymerases when encountering AFB_1-FAPY adducts. By comparing the qualitative *in vitro* bypass data, only pol ζ displayed the corresponding mutagenic bypass specificity for G to T transversions. These results also provided support for the mechanism of direct misinsertion/extension across the lesion by DNA polymerases, rather than the polymerase slippage model. Potentially, in the cellular context, there may be yet unknown accessory and/or regulatory proteins involved in facilitating the bypass process since the mutation was readily detected in the primate cells (Table I). Further studies are needed to examine this possibility.

Based on crystallographic studies, it has been proposed that the mutagenic bypass of AFB_1-FAPY may be due to the structural restriction for an incoming deoxycytidine triphosphate access. The conformation of the AFB_1 moiety within the active site of the polymerase Dpo4 appeared with a distinct orientation about the N^5-C8 bond of

the AFB_1-FAPY adduct (35). The rotation about the C5-N^5 the bond of the pyrimidinyl moiety allows the AFB_1 moiety to be parallel to the FAPY base since the N^5-C8 bond was out of plane, shifting to the 5′-direction in respect to the FAPY base. This led to a stronger stacking ability of AFB_1-FAPY, that may hinder the access of the incoming dNTP within the active site (35,47,48). However, a more detailed understanding of the mechanism of action of polymerases on AFB_1-FAPY adducts awaits the crystal structure of the cognate polymerase in complex with this lesion.

There are two anomers of AFB_1-FAPY, α and β forms at the deoxyribose, that have been detected in oligodeoxynucleotides (13,23). The equilibrium ratio of α:β is 2:1 in ss DNA. The β-anomer has been shown to be mutagenic in *E. coli*, in contrast to the α form, which acts as a replication block (23). Theoretically, the site-specific AFB_1-FAPY adducts in the ss pMS2 vector consisted of a mixture of α and β anomers; however, we could not determine which anomer induced each mutation in primate cells. Thus, although it is not yet known which form(s) of AFB_1-FAPY could be bypassed in mammalian cells, extrapolation of the data derived from the *E. coli* system would postulate that the mutagenic anomer would be in the β configuration.

In the present report, we demonstrate that the AFB_1-FAPY adduct is a biologically relevant DNA modification causing G to T transversions. We also provide biochemical evidence of DNA replication bypass of AFB_1-FAPY adducts. Insights gained from these biochemical studies have laid the foundation for *in vivo* assays that can elucidate the cellular pathways involved in replication bypass of AFB_1-FAPY adducts in mammalian cells. Our data suggest that pol ζ is the most likely TLS polymerase that is responsible for AFB_1-induced mutagenesis, which is believed to be the initiating event of AFB_1-associated HCC.

Supplementary material

Supplementary Figures 1 and 2 can be found at http://carcin.oxfordjournals.org/

Funding

National Institutes of Health (R01 CA055678 to M.P.S. and R.S.L., GM 032431 to P.M.B., P30 ES00267 to M.P.S.).

Acknowledgements

We thank Dr M.Moriya (State University of New York at Stony Brook) for the generous gift of pMS2 vector, Dr I.G.Minko for extensive consultations on these investigations and preparation of the ss pMS2, L.F.Earley for technical support and Dr R.Eoff for the generous gift of pol η catalytic core.

Conflict of Interest Statement: None declared.

References

1. Ferlay,J. *et al.* (2010) Estimates of worldwide burden of cancer in 2008: GLOBOCAN 2008. *Int. J. Cancer*, **127**, 2893–2917.
2. Kensler,T.W. *et al.* (2011) Aflatoxin: a 50-year odyssey of mechanistic and translational toxicology. *Toxicol. Sci.*, **120**, S28–S48.
3. Wu,H.-C. *et al.* (2012) The role of aflatoxins in hepatocellular carcinoma. *Hepatitis Monthly*, **12**, e7238.
4. Forrester,L.M. *et al.* (1990) Evidence for involvement of multiple forms of cytochrome P-450 in aflatoxin B_1 metabolism in human liver. *Proc. Natl Acad. Sci. USA*, **87**, 8306–8310.
5. Baertschi,S.W. *et al.* (1988) Preparation of the 8,9-epoxide of the mycotoxin aflatoxin B_1: the ultimate carcinogenic species. *J. Am. Chem. Soc.*, **110**, 7929–7931.
6. Martin,C.N. *et al.* (1977) Aflatoxin B-oxide generated by chemical or enzymic oxidation of aflatoxin B_1 causes guanine substitution in nucleic acids. *Nature*, **267**, 863–865.
7. Essigmann,J.M. *et al.* (1977) Structural identification of the major DNA adduct formed by aflatoxin B_1 *in vitro*. *Proc. Natl Acad. Sci. USA*, **74**, 1870–1874.
8. Lin,J.K. *et al.* (1977) 2, 3-Dihydro-2-(guan-7-yl)-3-hydroxy-aflatoxin B_1, a major acid hydrolysis product of aflatoxin B_1-DNA or-ribosomal RNA adducts formed in hepatic microsome-mediated reactions and in rat liver *in vivo*. *Cancer Res.*, **37**, 4430–4438.
9. Croy,R.G. *et al.* (1978) Identification of the principal aflatoxin B_1-DNA adduct formed *in vivo* in rat liver. *Proc .Natl Acad. Sci. USA*, **75**, 1745–1749.
10. Hertzog,P.J. *et al.* (1980) A high pressure liquid chromatography study on the removal of DNA-bound aflatoxin B_1 in rat liver and in vitro. *Carcinogenesis*, **1**, 787–793.
11. Croy,R.G. *et al.* (1981) Temporal patterns of covalent DNA adducts in rat liver after single and multiple doses of aflatoxin B_1. *Cancer Res*, **41**, 197–203.
12. Hertzog,P.J. *et al.* (1982) Characterisation of the imidazole ring-opened forms of trans-8,9-di-hydro-8-(7-guanyl)9-hydroxy aflatoxin B_1. *Carcinogenesis*, **3**, 723–725.
13. Brown,K.L. *et al.* (2006) Unraveling the aflatoxin-FAPY conundrum: structural basis for differential replicative processing of isomeric forms of the formamidopyrimidine-type DNA adduct of aflatoxin B_1. *J. Am. Chem. Soc.*, **128**, 15188–15199.
14. Foster,P.L. *et al.* (1983) Base substitution mutations induced by metabolically activated aflatoxin B_1. *Proc. Natl Acad. Sci. USA*, **80**, 2695–2698.
15. Chang,Y.J. *et al.* (1991) Analysis of ras gene mutations in rainbow trout liver tumors initiated by aflatoxin B_1. *Mol. Carcinog.*, **4**, 112–119.
16. Levy,D.D. *et al.* (1992) Sequence specificity of aflatoxin B_1-induced mutations in a plasmid replicated in xeroderma pigmentosum and DNA repair proficient human cells. *Cancer Res.*, **52**, 5668–5673.
17. Aguilar,F. *et al.* (1993) Aflatoxin B_1 induces the transversion of G-->T in codon 249 of the p53 tumor suppressor gene in human hepatocytes. *Proc. Natl Acad. Sci. USA*, **90**, 8586–8590.
18. Autrup,H. *et al.* (1996) Aflatoxin B_1 induced lacI mutation in liver and kidney of transgenic mice C57BL/6N: effect of phorone. *Mutagenesis*, **11**, 69–73.
19. Smela,M.E. *et al.* (2001) The chemistry and biology of aflatoxin B_1: from mutational spectrometry to carcinogenesis. *Carcinogenesis*, **22**, 535–545.
20. Hsu,I.C. *et al.* (1991) Mutational hotspot in the p53 gene in human hepatocellular carcinomas. *Nature*, **350**, 427–428.
21. Bressac,B. *et al.* (1991) Selective G to T mutations of p53 gene in hepatocellular carcinoma from southern Africa. *Nature*, **350**, 429–431.
22. Bailey,E.A. *et al.* (1996) Mutational properties of the primary aflatoxin B_1-DNA adduct. *Proc. Natl Acad. Sci. USA*, **93**, 1535–1539.
23. Smela,M.E. *et al.* (2002) The aflatoxin B_1 formamidopyrimidine adduct plays a major role in causing the types of mutations observed in human hepatocellular carcinoma. *Proc. Natl Acad. Sci. USA*, **99**, 6655–6660.
24. Waters,L.S. *et al.* (2009) Eukaryotic translesion polymerases and their roles and regulation in DNA damage tolerance. *Microbiol. Mol. Biol. Rev.*, **73**, 134–154.
25. Lange,S.S. *et al.* (2011) DNA polymerases and cancer. *Nat. Rev. Cancer*, **11**, 96–110.
26. Knobel,P.A. *et al.* (2011) Translesion DNA synthesis in the context of cancer research. *Cancer Cell. Int.*, **11**, 39.
27. Sale,J.E. *et al.* (2012) Y-family DNA polymerases and their role in tolerance of cellular DNA damage. *Nat. Rev. Mol. Cell. Biol.*, **13**, 141–152.
28. Yamanaka,K. *et al.* (2013) Functions of translesion DNA polymerases: Implications for cancer risk and opportunities as therapeutic targets. In Madhusudan,S. *et al.* (eds) *DNA Repair and Cancer: From Bench to clinic*. CRC press, pp. 325–371.
29. Prakash,S. (2002) Translesion DNA synthesis in eukaryotes: a one- or two-polymerase affair. *Genes Dev.*, **16**, 1872–1883.
30. Livneh,Z. *et al.* (2010) Multiple two-polymerase mechanisms in mammalian translesion DNA synthesis. *Cell Cycle*, **9**, 729–735.
31. Johnson,R.E. *et al.* (1999) Efficient bypass of a thymine-thymine dimer by yeast DNA polymerase, pol eta. *Science*, **283**, 1001–1004.
32. Johnson,R.E. (2000) Fidelity of human DNA polymerase eta. *J. Biol. Chem.*, **275**, 7447–7450.
33. Wang,Y. *et al.* (2007) Evidence that in xeroderma pigmentosum variant cells, which lack DNA polymerase eta, DNA polymerase iota causes the very high frequency and unique spectrum of UV-induced mutations. *Cancer Res.*, **67**, 3018–3026.
34. Ziv,O. *et al.* (2009) DNA polymerase zeta cooperates with polymerases kappa and iota in translesion DNA synthesis across pyrimidine photodimers in cells from XPV patients. *Proc. Natl Acad. Sci. USA*, **106**, 11552–11557.

35. Banerjee,S. *et al.* (2011) Bypass of aflatoxin B_1 adducts by the *Sulfolobus solfataricus* DNA polymerase IV. *J. Am. Chem. Soc.*, **133**, 12556–12568.
36. Jin,Y.H. *et al.* (2005) The multiple biological roles of the 3"->5" exonuclease of *Saccharomyces cerevisiae* DNA polymerase delta require switching between the polymerase and exonuclease domains. *Mol. Cell. Biol.*, **25**, 461–471.
37. Moriya,M. (1993) Single-stranded shuttle phagemid for mutagenesis studies in mammalian cells: 8-oxoguanine in DNA induces targeted G.C-->T.A transversions in simian kidney cells. *Proc. Natl Acad. Sci. USA*, **90**, 1122–1126.
38. Kanuri,M. *et al.* (2002) Error prone translesion synthesis past gamma-hydroxypropano deoxyguanosine, the primary acrolein-derived adduct in mammalian cells. *J. Biol. Chem.*, **277**, 18257–18265.
39. Minko,I.G. *et al.* (2008) Mutagenic potential of DNA-peptide crosslinks mediated by acrolein-derived DNA adducts. *Mutat. Res.*, **637**, 161–172.
40. Liu,Y. *et al.* (2010) Global burden of aflatoxin-induced hepatocellular carcinoma: a risk assessment. *Environ. Health Perspect.*, **118**, 818–824.
41. Fernandes,P.H. *et al.* (2006) Synthesis and mutagenesis of the butadiene-derived N3 2′-deoxyuridine adducts. *Chem. Res. Toxicol.*, **19**, 968–976.
42. Minko,I.G. *et al.* (2008) Role for DNA polymerase kappa in the processing of N2-N2-guanine interstrand cross-links. *J. Biol. Chem.*, **283**, 17075–17082.
43. Woo,L.L. *et al.* (2011) Aflatoxin B_1-DNA adduct formation and mutagenicity in livers of neonatal male and female B6C3F1 mice. *Toxicol. Sci.*, **122**, 38–44.
44. Riley,J. (1997) In vitro activation of the human Harvey-ras proto-oncogene by aflatoxin B_1. *Carcinogenesis*, **18**, 905–910.
45. Besaratinia,A. *et al.* (2009) In vitro recapitulating of TP53 mutagenesis in hepatocellular carcinoma associated with dietary aflatoxin B_1 exposure. *Gastroenterology*, **137**, 1127–37, 1137.e1–5.
46. Guo,Y. *et al.* (2005) Expression of a human cytochrome p450 in yeast permits analysis of pathways for response to and repair of aflatoxin-induced DNA damage. *Mol. Cell. Biol.*, **25**, 5823–5833.
47. Giri,I. *et al.* (2002) Thermal stabilization of the DNA duplex by adducts of aflatoxin B_1. *Biopolymers*, **65**, 190–201.
48. Brown,K.L. *et al.* (2009) Structural perturbations induced by the alpha-anomer of the aflatoxin B_1 formamidopyrimidine adduct in duplex and single-strand DNA. *J. Am. Chem. Soc.*, **131**, 16096–16107.

Received October, 2, 2013; revised December 18, 2013; accepted December 30, 2013